JOURNAL OF MATERIALS SCIENCE 37 (2002) 2305–2309

Synthesis of polymaleimide/silica nanocomposites

GUO TAO LU, YING HUANG*
The Center for Molecular Science, Institute of Chemistry, Chinese Academy of Sciences, Beijing 100080, People's Republic of China
E-mail: ying2huang@yahoo.com.cn

Polymaleimide/Silica nanocomposites were synthesized from *N*-γ-Triethoxysilylpropyl-maleamic acid (TESPMA) through sol-gel process, imidation reaction of the maleamic acid functional groups and thermal polymerization of the formed maleimide at elevated temperature. These nanocomposite materials were characterized by Fourier transform infrared analysis (FT-IR), differential scanning calorimetry (DSC), thermogravimetric analysis (TGA) and field emission scanning electron microscopy (FE-SEM). It was found that the inorganic networks chemically bound to polymaleimides enhanced the thermal stability of these nanocomposites greatly. Nevertheless, incorporation of colloidal silica did not make positive contributions to the thermal stability, although the weight fraction of the inorganic part in the composite was increased significantly.

1. Introduction

Organic-inorganic nanocomposite materials are of great research interest recently [1]. Because of their broad and potential applications in electronics, optics, chemistry and biomedicine, a great deal of research work in this area has been performed in recent years [2–6].

The sol-gel process has been widely used for preparation of organic-inorganic nanocomposite materials. There are several advantages in using sol-gel chemistry, including the low synthesis temperature, easiness of obtaining optically transparent nanocomposites, versatility of control over the nature of the organic-inorganic interface, as well as convenience of introducing new properties into the resulting materials [6].

Two different approaches have been employed for synthesis of organic-inorganic nanocomposites by sol-gel process. Nano-particles of metal oxide can be synthesized in the presence of a pre-formed organic polymer [7–9]. Alternatively, the sol gel synthesis is carried out in an organic monomer that is polymerized subsequently or concurrently [10–12]. According to the nature of the interfacial interaction, the resulting nanocomposite materials can be classified into two categories: class 1, nanocomposites with interfacial covalent bonds between the organic and inorganic phases [13, 14]; class 2, nanocomposites without covalent bonds between the two phases, only with hydrogen bonds between them [15–17].

Since inorganic materials are intrinsically more thermo-stable than organic polymers, inorganic nanophase is introduced to improve the heat resistance of organic polymers. Hybrid materials of polyacrylates [18], polymethacrylates [15], polyacrylonitrile [8], polyvinyl acetate [16], polystyrene[14], maleimide-styrene copolymers [19], polycarbonate [20], epoxy resins [21] and polyimides [17] have been studied. Polymaleimide is thermally very stable [22]. In this paper we report the synthesis of polymaleimide/silica nanocomposite materials by a sol gel process. *N*-γ-triethoxysilylpropyl-maleamic acid was prepared, and its hydrolytic condensation was carried out in the presence or absence of colloidal silica. Ring-closing reaction of the maleamic acid as well as thermopolymerization of the formed maleimide were effected at elevated temperatures. FT-IR, DSC, TGA and FE-SEM were used to characterize the hybrid materials.

2. Experimental

2.1. Materials

Maleic anhydride (MAH) was an analytical reagent of purity 99.5%. The aqueous colloidal silica with 30 wt% silica and 12.6 nm average particle size was provided by the Haiyang Chemical Factory of Tsingdao, China. γ-Aminopropyltriethoxy-silane (APTES) from the Gaixian Secondary Chemical Factory, China was purified by fractional distillation under reduced pressure. Tetrahydrofuran (THF) was analytic reagent from the Beijing Chemical Factory, China. It was purified by refluxing over $Na/CO(C_6H_5)_2$ and distillation. Hydrochloric acid (35–38%) and glacial acetic acid were analytic reagents.

2.2. Synthesis of *N*-γ-triethoxysilylpropyl-maleamic acid (TESPMA)

N-γ-triethoxysilylpropyl-maleamic acid (TESPMA) was prepared through aminolysis reaction of maleic

*Author to whom all correspondence should be addressed.

anhydride with APTES in the molar ratio 1:1 with purified THF as solvent. For example, 110.63 g (0.50 mol) of APTES was weighed into a three-neck round flask equipped with a mechanical stirrer, a nitrogen inlet and a condenser with a nitrogen outlet on its top. The flask was flushed with high purity nitrogen. 20×10^{-6} m^3 THF was added, and then 49.03 g (0.5 mol) of maleic anhydride was introduced in several portions under stirring. After completion of the addition, the reaction mixture was stirred for 4 h to give a pale-yellow transparent solution of TESPMA in THF. The resultant solution was kept in a desiccator before using. Completion of the aminolysis reaction was indicated by FT-IR and ^{1}H-NMR ($CDCl_3$) spectra of the TESPMA product.

2.3. Preparation of the polymaleimide (PMI)/silica nanocomposites

The aqueous colloidal silica was acidified to pH 4 by adding a suitable amount of hydrochloric acid. 7.97 g of the solution of TESPMA in THF (containing 0.02 mol TESPMA) was mixed with a prescribed amount of the acidified aqueous colloid silica in a 50×10^{-6} m^3 conical flask under magnetic stirring for 30 min to give a transparent solution. The solution was stirred at room temperature for an additional 24 h and then transferred into a 50×10^{-6} m^3 beaker. The beaker was capped with aluminum foil, on which a number of small pinholes were made. Then the beaker was heated in an oil bath at 70°C for 10 days to remove the solvent, water and reaction byproducts slowly. A transparent pale-yellow monolith solid, termed as ORMOSIL was obtained. It was treated by heating in an oven from 80°C to 200°C with a step-by-step procedure. The PMI/silica nanocomposites thus obtained were red transparent glass. The compositions of the PMI/SiO_2 nanocomposites were shown in Table I.

TABLE I The composition of the PMI/silica nanocomposites

Sample code	Organic phase (wt%)	$SiO_{3/2}$ (wt%)	Colloidal silica (wt%)	Total inorganic phase (wt%)
PMI/SIL-27-0	72.6	27.4	0	27.4
PMI/SIL-38-14	62.4	23.5	14.1	37.6
PMI/SIL-43-22	57.0	21.5	21.5	43.0
PMI/SIL-53-35	46.9	17.7	35.4	53.1

2.4. Measurements

^{1}H NMR spectra were obtained with a Bruker MW 300 spectrometer with $CDCl_3$ as solvent. FT-IR spectra were recorded on a Perkin-Elmer model 1600 IR spectrometer. Thermogravimetric analysis (TGA) was performed on a Perkin-Elmer TGA-7 thermogravimeter with a heating rate of 20°C/min under a nitrogen flow rate of 10^{-4} m^3/min. Differential scanning calorimetry (DSC) was performed on a Perkin-Elmer DSC-7 differential scanning calorimeter at a heating rate 20°C/min and nitrogen flow 10^{-4} m^3/min. The microstructure features of the nanocomposite materials were examined with a Hitachi S-900 field emission scanning electron microscope.

3. Results and Discussion

3.1. Synthesis of polymaleimide/silica nanocomposites

The reactions involved in the synthesis of polymaleimide/silica nanocomposites are shown in Schemes 1 and 2. The first step of the synthesis was a sol-gel process of TESPMA with or without colloidal silica under the catalysis of acid, producing an ormosil with potentially polymerizable groups. It was then treated by heating in an oven from 80°C to 200°C with a step-by-step procedure to give the nanocomposite. In this process the imide rings formed

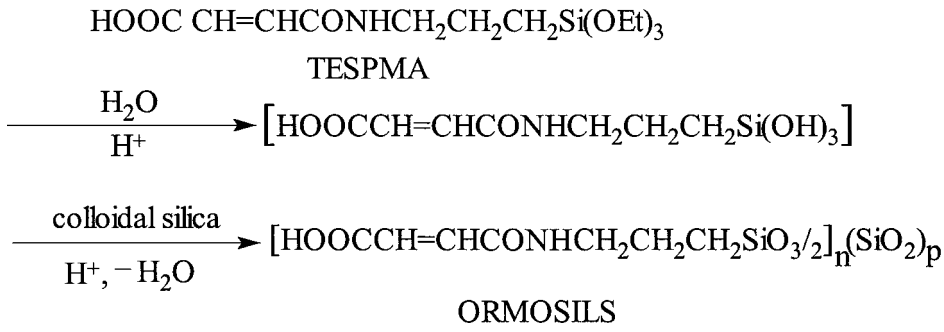

Scheme 1 Reactions in the sol-gel process.

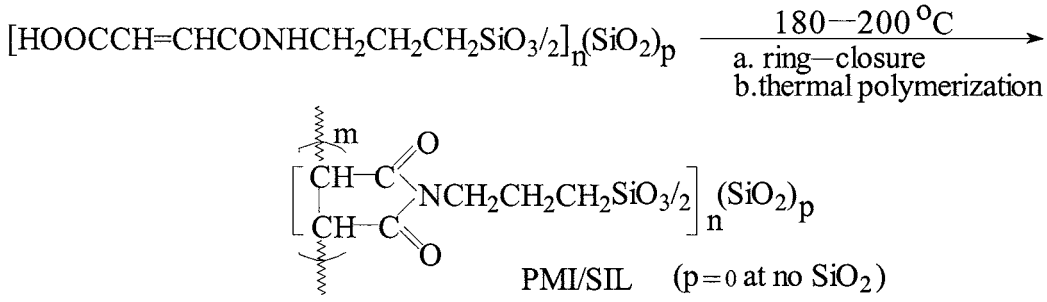

Scheme 2 Reactions in the thermal treatment.

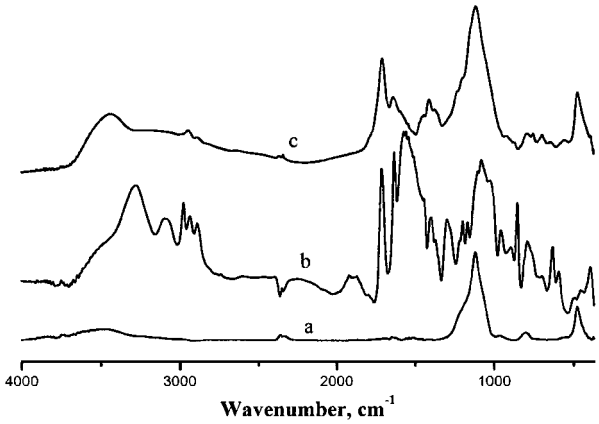

Figure 1 FT-IR spectra for (a) silica sol, (b) TESPMA and (c) the ormosil-43-22.

and the polymerization of the maleimide groups took place.

The changes were studied by IR spectroscopy. A FT-IR spectrum for the ormosil-43-22 is shown in Fig. 1. The spectra of TESPMA and silica sol are also given in Fig. 1 for comparison. It is seen that the absorptions at 852 cm^{-1}, 956 cm^{-1}, 1080 cm^{-1} and 1166 cm^{-1} from the Si─OC_2H_5 groups, and the peaks at 2975 cm^{-1} and 2886 cm^{-1} from the stretching vibration of ─CH_3 in the Si─OC_2H_5 group completely disappeared after the sol-gel process. At the same time, new absorptions at 919 cm^{-1} and 3420 cm^{-1} by the Si─OH groups appeared and the broad peak at 1078 cm^{-1} was shifted to 1114 cm^{-1}. All these changes indicated that the ethoxy groups bound to silicon atoms were completely hydrolyzed and transformed into silanols. Meanwhile, the latter condensed with each other and with the silanol groups on the surface of the colloidal silica particles to form Si─O─Si bonds.

The ring closure reaction of the maleamic acid was also proceeded to some extent in the ormosil, as shown by the remarkable reduction of the absorbance at 1634 cm^{-1}, 1555 cm^{-1}, 1297 cm^{-1} and 3277 cm^{-1} from amide groups in the spectrum for the ormosil compared with the spectrum for TESPMA.

The second step for the synthesis of the PMI/silica nanocomposites was the thermal treatment of the ormosils. Fig. 2 compares the FT-IR spectra for the ormosil-43-22 and the corresponding nanocomposite after the thermal treatment. It is seen in Fig. 2 that the absorption peaks at 1632 cm^{-1}, 1555 cm^{-1}, 1297 cm^{-1} and 3277 cm^{-1} from amide groups as well as the peak at 1711 cm^{-1} from the carboxyl groups of maleamic acid disappeared and two new absorption peaks at 1704 cm^{-1} and 1778 cm^{-1} characteristic of the maleimide groups appeared. In addition, the absorption peak at 3080 cm^{-1} from the double bond of maleimide became extremely weak after the thermal treatment, indicating the polymerization of the unsaturated group of the maleimide.

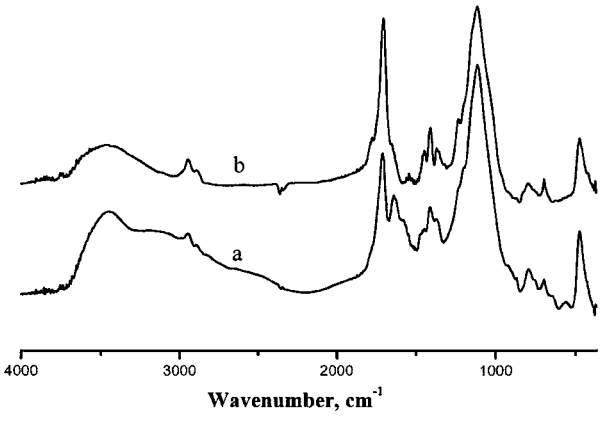

Figure 2 FT-IR spectra for (a) the ormosil-43-22 before thermal treatment and (b) the PMI/SIL-43-22 after thermal treatment.

The adsorption peaks at 919 cm^{-1} and 3422 cm^{-1} from Si─OH attenuated remarkably during thermal treatment, indicating the condensation of Si─OH groups to form the more perfect Si─O─Si network in the PMI/silica nanocomposite.

3.2. Morphology of the PMI/silica nanocomposites

All the PMI/silica nanocomposites listed in Table I are red and transparent glass. The FE-SEM photographs of the fracture surfaces (Fig. 3) indicate that they are two-phase materials microscopically. It can be seen in Fig. 3a that in the nanocomposite PMI/SIL-27-0 (without addition of colloidal silica) the inorganic phase formed discrete domains with a narrow particle size distribution in the range of 10–20 nm. Aggregates with the size greater than 20 nm were very few. As colloidal silica was incorporated into the inorganic phase of the PMI/silica nanocomposites, however, the particle size of the inorganic phase in the nanocomposites became obviously larger. In the nanocomposites PMI/SIL-53-35, a great deal of particle aggregates in the range 30–60 nm and a few bigger aggregates greater than 60 nm were formed.

3.3. Thermal stability of the PMI/silica nanocomposites

The thermal properties of the PMI/silica nanocomposites were studied using DSC and TGA. The glass transition temperatures (T_g) of the PMI/silica nanocomposites determined by DSC are listed in Table II. In comparison with the T_g 185°C for the *N*-butyl-substituted polymaleimides [23], a substantial improvement in T_g was achieved in the nanocomposites PMI /SIL-27-0. As the fraction of the inorganic phase was increased by incorporation of colloidal silica, the T_g enhanced still further.

TABLE II Thermal properties of PMI/silica nanocomposites (TGA : 20°C/min, N_2)

Sample code	T_g (°C)	5 wt% loss temp (°C)	10 wt% loss temp (°C)	$T_{max.}$ (°C)	Wt. retention @ 700°C (%)
PMI/SIL-27-0	254	390	467	561	57.8
PMI/SIL-38-14	278	365	446	525	64.5
PMI/SIL-43-22	282	377	468	554	68.3
PMI/SIL-53-35	284	372	468	531	71.1
PMI[21]	–	–	–	426	–
PBMI[22,23]	185	–	–	403	–

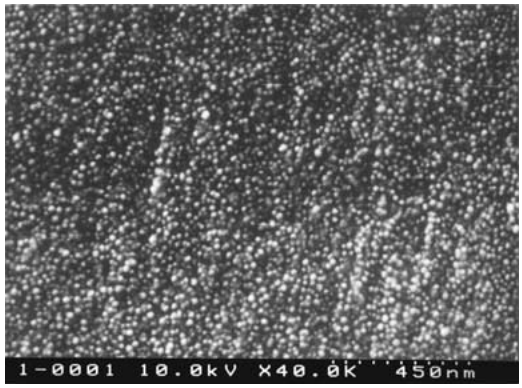

(a)

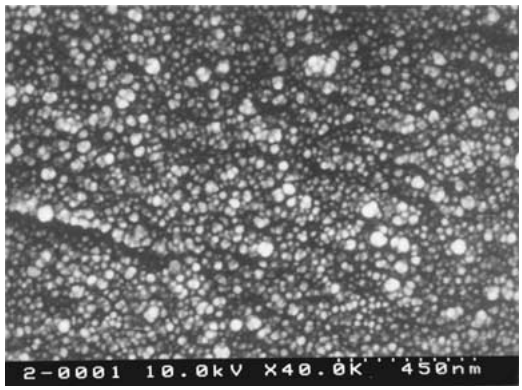

(b)

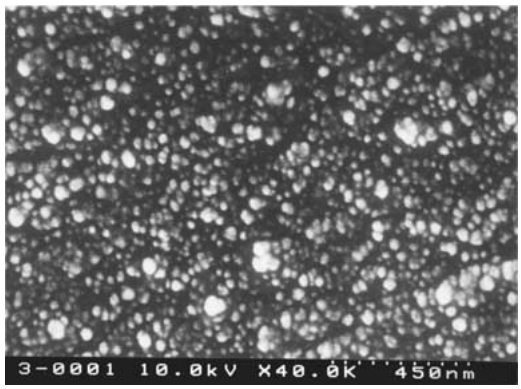

(c)

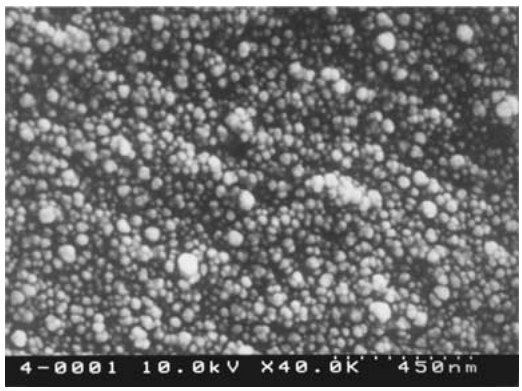

(d)

Figure 3 FE-SEM photographs for PMI/silica nanocomposites (magnification × 40.0k): (a) PMI/SIL-27-0, (b) PMI/SIL-38-14, (c) PMI/SIL-43-22 and (d) PMI/SIL-53-35.

Fig. 4 gives the TGA diagrams for the PMI/silica nanocomposites with different inorganic content. As shown in Fig. 4, the weight-loss process of these nanocomposites was in two steps. The minor weight losses beginning at 150°C were attributed to the elimination of water produced by further condensation between residual Si─OH and the ring closure reaction of the residual maleamic acid functional groups. The major weight loss occurred at >450°C, which was caused by decomposition of the organic polymer in these PMI/silica nanocomposites. The temperatures of 5% weight loss and 10% weight loss and the maximum decomposition temperatures (T_{max}) in the TGA diagrams are summarized in Table II, with some results of *N*-alkyl-substituted polymaleimides [22] for comparison. It is seen from Table II that T_{max} of all the nanocomposites are substantially higher than those for *N*-alkyl-substituted polymaleimides.

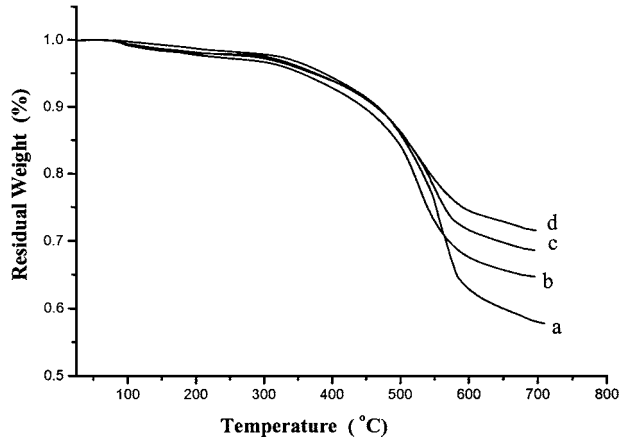

Figure 4 TGA diagrams for PMI/silica nanocomposites: (a) PMI/SIL-27-0, (b) PMI/SIL-38-14, (c) PMI/SIL-43-22 and (d) PMI/SIL-53-35.

It is noteworthy that the inorganic networks chemically bound to polymaleimides worked well for improving the thermal resistance of the nanocomposites. The nanocomposite PMI/SIL-27-0 (without colloidal silica) showed the highest value of T_{max}. In contrast, incorporation of colloidal silica did not make positive contributions to the thermal stability, although the weight fraction of the inorganic part in the composite was increased significantly.

4. Conclusions

Transparent PMI/silica nanocomposites were synthesized from *N*-γ-Triethoxysilylpropyl-maleamic acid by sol-gel process with or without colloidal silica, ring-closure reaction of the maleamic acid and thermopolymerization of the formed maleimide at elevated temperatures. The average particle size of the inorganic phase in these nanocomposites was in the range of 10–40 nm. These PMI/silica nanocomposites showed excellent thermal stability: high glass transition temperature and high decomposition temperatures. The results indicate that the inorganic networks chemically bound to polymaleimides enhanced the thermal stability of these nanocomposites. Incorporation of colloidal silica did not make positive contributions to the thermal stability, although the weight fraction of inorganic part in the composite was increased significantly.

References

1. W. BOLTON, in "Engineering Materials Pocket Book" (CRC Press, Baton Rouge, 1989) p. 171.
2. M. J. MACLACHLAN, I. MANNERS and G. A. OZIN, *Adv. Mater.* **12** (2000) 675.
3. M. W. ELLSWORTH and D. L. GIN, *Polym. News* **24** (1999) 331.
4. L. L. HENCH and J. K. WEST, *Chem. Rev.* **90** (1990) 33.
5. B. M. NOVAK, *Adv. Mater.* **5** (1993) 422.
6. J. WEN and G. WILKES, *Chem. Mater.* **8** (1996) 1667.
7. C. DENG, P. F. JAMES and P. V. WRIGHT, *J. Mater. Chem.* **8** (1998) 153.
8. Y. WEI, D. C. YANG and L. G. TANG, *Makromol. Chem. Rapid Commun.* **14** (1993) 273.
9. S. S. SHOJAIE, T. G. RIALS and S. S. KELLEY, *J. Appl. Polym. Sci.* **58** (1995) 1263.
10. H. SCHMIDT, *J. Non-Cryst. Solids* **112** (1989) 419.
11. M. W. ELLSWORTH and B. M. NOVAK, *J. Am. Chem. Soc.* **113** (1991) 1756.
12. B. M. NOVAK and C. DAVIS, *Macromols.* **24** (1991) 5481.
13. H. B. SUNKARA, J. M. JETHMALANI and W. T. FORD, *Chem. Mater.* **6** (1994) 362.
14. T. H. MOUREY, S. M. MILLER, J. A. WESSON, T. E. LONG and L. W. KELTS, *Macromolecules* **25** (1992) 45.
15. E. J. POPE, M. ASAMI and J. D. MACKENZIE, *J. Mater. Res.* **4** (1989) 1017.
16. C. J. LANDRY and B. K. COLTRAIN, *J. Macromol. Sci. Pure Appl. Chem.* A **31** (1994) 1965.
17. A. MORIKAWA, H. YAMAGUCHI, M. KAKIMOTO and Y. IMAI, *Chem. Mater.* **6** (1994) 913.
18. Y. WEI, W. WANG, D. YANG and L. TANG, *ibid.* **6** (1994) 1737.
19. R. M. SHALTOUT, D. A. LOY and D. R. WHEELER, *Mat. Res. Soc. Symp. Proc.* **576** (1999) 15.
20. C. J. T. LANDRY and B. K. COLTRAIN, *Polym. Prepr.* **32** (1990) 514.
21. B. MESSERSMITH and E. P. GIANNELIS, *Chem. Mater.* **6** (1994) 1719.
22. T. OTSU, A. MATSUMOTO, T. KUBOTA and S. MARI, *Polym. Bull.* **23** (1990) 43.
23. A. MATSUMOTO, Y. OKI and T. OTSU, *Polym. J.* **23** (1991) 201.

Received 11 June 2001
and accepted 11 February 2002